ISBN: 978-3-95450-192-2 doi:10.18429/JACoW-IBIC2017-WEPCC13

PRELIMINARY STUDY ON IPM FOR CADS INJECTOR I*

J. He†, Z. Z. Wang, J. S. Zhou, Y. F. Sui, J. H. Yue, J. S. Cao
Key Laboratory of Particle Acceleration Physics & Technology,
Institute of High Energy Physics, Beijing 100049, China

Abstract

The Ionization Profile Monitor (IPM) based on the residual gas molecule is designed and fabricated for high power proton beam accelerator China Accelerator Driven Subcritical system injector I. The method of calculating the intensity of ionization signal is explored. The device uses the electric field generated by electrode to guide the ions, using Microchannel plates (MCP) to amplify ionization signals. A screen and a camera is used to detect the output electrons of the MCP, which present the distribution of the beam. The electric field distribution is optimized by CST ELECTROMAGNETIC STUDIO calculation. The IPM is installed on the ADS injector I and tested by beam. It measures the proton profile successfully during the CW commission. The experiment results agree well with the theoretical value which proves that the equipment can be used for CADS main linac in future.

INTRODUCTION

The Ionization Profile Monitor (IPM), also known as Residual Gas Monitor (RGM), is one of the most popular non-destructive profile detection device, mainly used for the machine which the beam size is in the range from mm to cm. High intensity and high power hadron accelerators usually implies the usage of non-destructive methods[1]. For the high power beam, the interception materials such as the phosphor screen [2], the wire target [3], the secondary electron grid may be damaged by the beam. Laser scanning [4], electron beam scanning [5] and residual gas detectors will not have this problem. There are a lot of IPM research experience in different lab, such as FNL [6, 7], KEK [8, 9], BNL [10], and CERN [11]. Several IPM systems have been installed and several workshops focus on this topic have been held in GSI [12, 13, and 14].

With the development of China high-power proton accelerator, there is a growing demand for non-destructive profile detection, such as Chinese Spallation Neutron Sources (CSNS) and Accelerator Driven Subcritical systems (ADS). There are several wires have been destroyed by beam both in CSNS and ADS. Two non-invasive beam profile measurement methods were developed including the electron scanner and IPM on ADS Injector I. The Fig.1 (a) shows the layout of the injector and the locations of both electron scanner and IPM. The Fig.1 (b) shows the RMS beam size from the exit of the ion source to the dump, the blue curve is the horizontal size and the red curve is vertical size. As shown in Fig. 1 (b), the theoretical beam size at the IPM location is 15 mm × 5mm.

The most important parameters that affects IPM systems is the ionization yield, which is how much electron-ion pairs are generated per second. It is determined by the beam parameters and the vacuum parameters, including the pressure and the composition of the residual gas. The Bethe-Bloch formula describes the energy loss caused by the collision between the beam and residual gas which is related to the energy of the beam. The total ionization number N can be expressed as: $N=\Delta E/I_0$, where the ΔE is the total energy loss in the gas volume, and I_0 is the average energy required to produce an electron-ion pair, also known as ionization energy, usually is about 20~30 eV. According $N_D = (-dE/dx)\cdot l \cdot I_{current} / I_0$, for the ADS beam, $I_{current}$=10 mA, assume that the residual gas is H_2 and the pressure is 1×10^{-5} Pa, the detector longitudinal length l = 3 cm, I_0 = 33 eV, the N_D is 3.86 x 10^7 pps for CW beam.

EXPERIMENT

The experiment set up is shown as Fig. 2. The device is working in ion collection mode. In order to produce a guild field of 1 kV / cm, ±4 kV is applied to the upper and lower oxygen-free copper electrodes, respectively.

Table 1: IPM Design Parameters for ADS Injector I

Parameters	Value
Electric field（V/m）	10^5
Distance of two plates（cm）	8
Size of MCP（mm）	Φ75
Size of EGA (mm)	Φ70
Detector	P43 +CCD
Work mode	Ions
Magnetic field	0

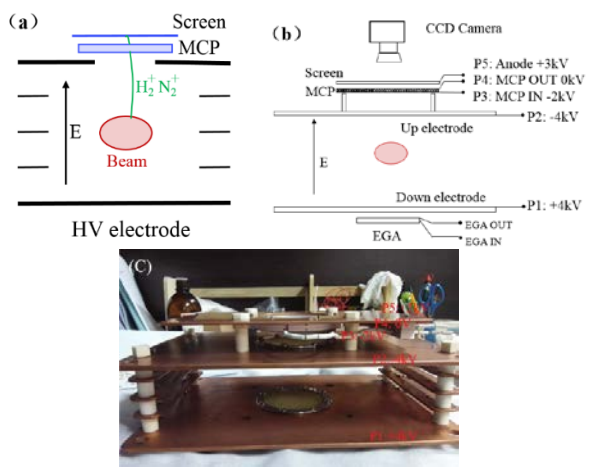

Figure 2: (a) Schematic of ion collection by E-field IPM (b) potential distribution MAP of IPM different components (c) picture of Oxygen-free copper electrodes and MCP.

* Work supported by the NSFC under grant No.11305186
† hejun@ihep.ac.cn

ISBN: 978-3-95450-192-2 doi:10.18429/JACoW-IBIC2017-WEPCC13

The distance of the two electrodes is 8 cm. The potential of other components is shown in Fig. 2 (b). The MCP is a two-stage V type with a nominal gain of 10^5, the potential difference between the output and input of the MCP is 2 kV as shown in Fig. 2 (b). The potential difference between the MCP out and the anode phosphor screen is 3 kV which to allow the MCP output electrons to be accelerated and hit the screen to produce photons, EGA from the PHOTONIS company has not been installed at this stage, it will adding to the device in future. The photo of the electrode and MCP are shown in Fig. 2 (c), there are two nets made by brass with a transmittance of 90% in the upper and lower electrodes. The design parameters are shown in Table 1.

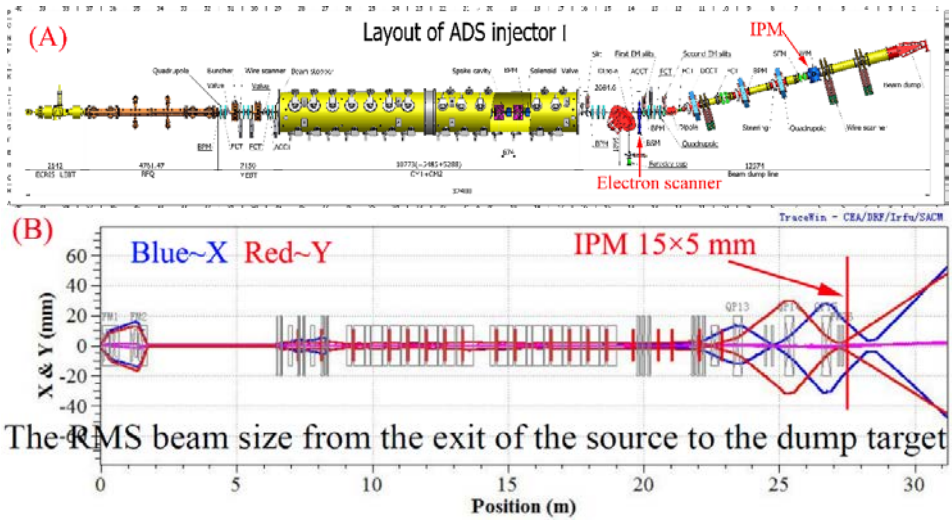

Figure 1: (a) the layout of ADS Injector I and the location of the non-invasive profile measurement (b) Beam size of the Injector I, 15×5mm at the IPM location.

In order to ensure that the generated ions (from initial ionization position to the detector) travel along the straight line, a higher and uniform Ey is better. (As shown in Fig. 3, assume horizontal direction is x, the vertical direction is y, longitudinal direction is z). The six small electrodes are helping to get a more uniform field. The two holes make the E-field worse in the centre of the electrode, it will be better after adding the brass nets and small electrodes as shown in Fig. 3 (a) and Fig. 3 (b). Fig. 3 (c) shows the Ey of the centre line (black curve) as shown in Fig. 3 (b). Small electrodes are connected with a 10 MΩ resistance. To increase the number of small electrodes, increase the size of the entire electrode x direction can improve the central area Ex, the electrode longitudinal size has little effect on the Ex, but can slightly improve the uniformity of Ey.

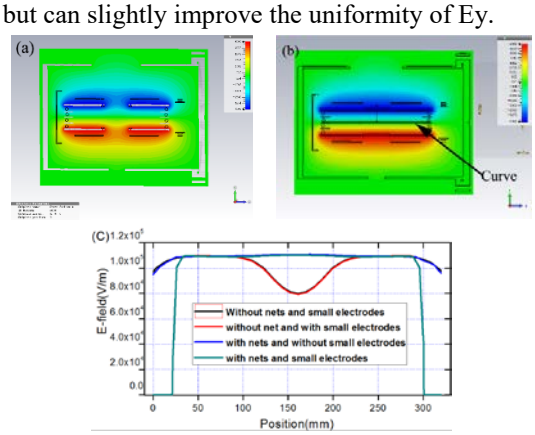

Figure 3: (a) The distribution of equal potential curve in my plane without the net (b) with the net (c) Ey in the Z direction (as shown in Fig. 3 (b).

Figure 4 shows the mechanical design and photos of the IPM system. Fig. 4 (a) is a mechanical design. The size of the large electrode is 320 mm × 220 mm × 3 mm, the size of the small electrode is 180 mm × 30 mm × 3 mm, the electrodes are supported and insulated with ceramics, and the longitudinal size of system is 450 mm. The image is recorded by an industrial camera with a resolution of 1360 × 1024, the pixel size of the sensor is 5.3 μm × 5.3 μm. With an external trigger function, it can simultaneous exposure with beam. The after time of P43 phosphor screen is 1ms from 90% to 10%, is 1.6 ms from 10% to 1%

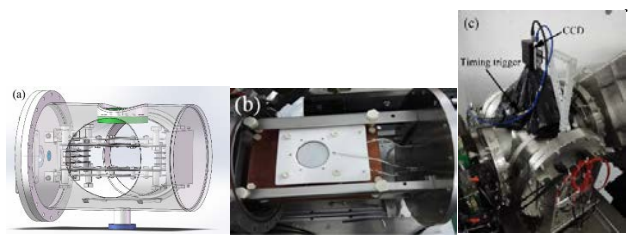

Figure 4: The Ionization profile monitor system, (a) mechanical design, (b) interior photos, (c) exterior photos.

Figure 5 is IPM system measurement results. Figure 5 (a) is the screen image before adding a cover, the shadow in the centre is produce by the CCD camera and bracket, it will remove after adding the black cloth shield as shown in Figure 4 (c). Figure 5 (b) is a pseudo-colour image of the screen with a duty factor of 10% proton beam after the stray light is masked. The time from camera receiving the trigger signal to stat to exposure is about 3 μs. The cable delay are in ns range and the afterglow time of the screen is 2~3 ms. the digital delay generator (DG645)

ISBN: 978-3-95450-192-2 doi:10.18429/JACoW-IBIC2017-WEPCC13

is used to control the exposure time synchronize with the beam. The Figure 5 (c) is the profile Gaussian fitting results. The dash line is the summation along the horizontal in the area in Figure 5 (b) indicate by the red lines. The RMS width is 13.72 mm ± 0.28 mm, which is close to the theoretical value of 15 mm. The result is worse in the lower duty ratio (<1%). The deviation from the Gaussian distribution is mainly due to the synchronization of the exposure time, the afterglow time and the beam are not exactly matched.

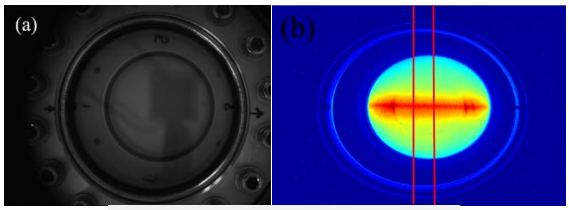

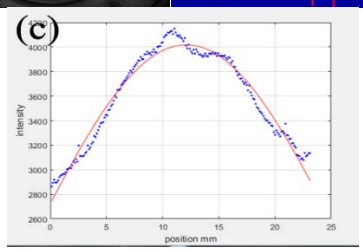

Figure 5: Results of IPM measurement. (a) Picture of screen without a beam, (b) picture of screen with a 10% duty factor beam, (c) horizontal profile by fitting the curve with Gaussian.

CONCLUSION

A In order to measure the profile of proton of CADS which will operated in a CW mode, two noninvasive beam profile measurement methods were developed. The paper mainly introduces the results of IPM system, including the mechanical design and fabrication. The CST calculation is used for optimize the guide E-field, the effect of adding small electrodes and metal net is shown. In addition, the method of assessing the intensity of ionization signals based on beam and vacuum parameters are also studied. The experiment details, such as the potential distribution, the 2-stage MCP, optical system, calibration system EGA are also introduced. Finally, the IPM system have been installed on the ADS injector I, the beam measurement shows the results agreement with the theoretical expectation very well. The possible reason of the no-Gaussian distribution in a low duty factor is the synchronization is not perfect and the noise ratio is not good enough. Further study is under the way of this problem. Experiment results show that IPM is an effective method to measure the transverse profile a high power proton beam, and it will play an important role in the following projects such as CSNS and CIADS.

ACKNOWLEDGEMENT

The author thanks the experts in KEK and GSI for valuable discussion.

REFERENCES

[1] P. Forck. Lecture Notes on Beam Instrumentation and Diagnostics. CERN Accelerator school beam diagnostics 2016 and P. Forck" in *Proc. IPAC'2010*, pp.1261.
[2] Bravin E. Transverse beam profile. CERN Accelerator school beam diagnostics 2009.
[3] Y.F. Sui, H. Z. Ma, J. S. Cao, et al. Chinese Physics C, 2008, 32(5):397-399.
[4] J. He, C. Zhang, Q. Y. Deng, et al. "High Power Laser and Particle Beams 2015", 27(6):065103
[5] W. Blokland, Cousineau S. in *Proc. IPAC'2011*, pp.1438
[6] Denton K M. Philip A, David C, et al. in *Proc. IPAC'2011*, pp. 519-521.
[7] J. Zagel, A. Jansson, T. Meyer, et al. in *Proc. IBIC'2010,* pp. 111-115.
[8] K. Satou, S. Lee, T. Toyama, et al. in *Proc. EPAC'2008*, pp. 1275-1277.
[9] K. Satou, S. Lee S, T. Toyama, et al. in *Proc. HB'2010*, pp. 506-508.
[10] R. Connolly, J. Fite, S. Jao, et al. in *Proc. IBIC'2010,* pp. 116-118.
[11] C. Bal, V. Prieto, R. Sautier, et al. in *Proc. DIPAC'2007*, pp. 120-122.
[12] T. Giacomini T, P. Forck, D. Liakin, et al. in *Proc. DIPAC'2011*, pp. 419-421.
[13] C. Bohme, J. Dietrich, P. Forck, et al. in *Proc. DIPAC'2009*, pp. 191-193.
[14] http://indico.gsi.de/event/5366/